Leveraging PLOAM Messaging for Environmental Temperature Mapping in Aerial-deployed TDMA PON Networks

BORJA VIDAL*, CRISTIAN SALGADO-CAZORLA

[1] *Nanophotonics Technology Center, Universitat Politecnica de Valencia, Valencia, 46022, Spain*
**bvidal@dcom.upv.es*

Abstract: The use of optical access networks with aerial-deployed fiber for deriving maps of environmental temperature is investigated. Telecom operators have thousands of km of deployed fiber to provide last-mile broadband services, which could be leveraged to extract temperature information with no additional cost since data is already available as part of the physical layer operations, administration, and maintenance (PLOAM) traffic. Here, it is shown how this information can be used to develop maps of environmental temperature as a method to complement present weather observation platforms. Preliminary experimental results with a G.984 PON network in operation show the feasibility of the technique.

1. Introduction

Time-division multiplexing passive optical networks (TDM-PONs) have become ubiquitous in recent decades, mostly displacing technologies such as hybrid fiber-coax networks, xDSL, and wireless standards such as WiMAX. Thanks to the ability of TDM-PON equipment to provide bitrates well beyond the current needs of residential subscribers, the potential of optical fiber to be a future-proof access infrastructure, and the strong cost reductions in both OPEX and CAPEX in the last years, the number of FTTH subscribers will soon approach one billion, making optical access a mature communications technology.

The aim of this work is to study a new application of FTTH infrastructure in the framework of current efforts to integrate sensing capabilities into communications networks. In wireless communications, efforts are being devoted to developing multifunctional radio systems, known as joint communications and sensing (JCAS). They will provide new functionalities and, therefore, new sources of revenue for the infrastructure that telecom operators deploy. JCAS currently focuses on wireless systems, such as future cellular networks expanding sensing beyond subscriber positioning to radar-like features and environmental monitoring [1-2]. This concept has been recently expanded to optical transport networks for earthquake detection [3] and environmental sensing [4]. This approach offers an alternative to the traditional deployment of optical fiber distributed sensors [5] based on light scattering, which needs specific interrogator hardware to be added to the optical link edges as, for example, the use of optical fibers deployed on the electrical powerline grid to monitor physical damage, extreme weather or electrical faults.

In particular, here we investigate if the optical distribution network in FTTH, especially in aerially deployed networks, could be leveraged to extract estimations of the average environmental temperatures from information of the physical layer operations, administration, and management (PLOAM) overhead in TDMA PON standards, such as ITU-T G.984, ITU-T G.987, etc. This information is already available to network operators and can be mined with only small changes in the OLT control software. This will pave the way for developing a new functionality of FTTH networks, which will convert the access network into a large-scale distributed sensor just from the data signals transported in the communication network.

At present, national weather services gather meteorological information through different platforms. First, discrete weather stations are strategically located throughout the urban area. However, they provide only weather information about the surroundings where it is located, not detailed maps of temperature distribution throughout the city. A different approach relies on space-based instruments that can record temperature from satellites using various remote sensing techniques. Satellites equipped with thermal infrared (8-14 μm) instruments can retrieve land surface temperature remotely with amazing resolution by measuring radiation intensity at different wavelengths. Space missions such as ECOSTRESS or Sentinel-3 record Earth's temperature in this way. However, these space instruments provide land-surface temperature rather than air temperature, as given in weather forecasts. Additionally, satellite temperature measurements require precise calibration and validation. This involves comparing satellite observations with ground-based temperature measurements to ensure accuracy, such as weather stations, radiosondes (weather balloons), and other instruments. On the other hand, cloud cover and atmospheric conditions can affect the ability of temperature monitoring satellites to obtain clear measurements

Developing temperature maps of cities can contribute to a better understanding of urban meteorology and provide governments with enhanced awareness of urban conditions, for example, in relation to the identification and monitoring of areas of urban heat stress, which are gaining in relevance due to the more frequent and more intense heat waves caused by climate change. In some regions, network operators must often utilize underground channelization to deploy cables due to regulatory requirements to minimize visual and environmental impacts and enhance infrastructure resilience. Still, aerial cables are used in suburban and rural areas. Temperature information in these areas is also valuable since it can refine climate models due to the sparsity of sensors in these areas. It can have an impact in enhancing weather forecasts as recently has started to be done with GPS signals to improve humidity data [6].

This paper addresses the challenge of leveraging already deployed telecom infrastructure to develop temperature maps within cities and rural areas served by FTTH infrastructure, which is becoming more common. It has the advantage of relying on already deployed infrastructure; it requires no additional hardware, while software changes can be minimal. This means that the development of this new functionality of optical access networks would be basically cost-free, unlike satellite platforms, which require large budgets and are available for a few years. Additionally, it allows almost real-time temperature monitoring with the potential to provide good spatial resolution thanks to the dense deployment of FTTH networks. This information can interest city planners as a method to monitor heat stress continuously. Thus, it could become a new source of revenue for telecom operators. Weather forecast models benefit when more information with smaller spatial bins is added. Thus, optical networks can contribute to refining the accuracy of weather forecasting. The authors previously published a preliminary study on the potential of an FTTH link as a temperature sensor [7].

The remainder of the paper is organized as follows. Section 2 presents the approach to retrieving temperature information from PLOAM data. Section 3 introduces an algorithm for converting the temperature information of the link into a spatial temperature map and shows simulation results. Section 4 presents preliminary validation experiments performed over a commercial FTTH network in operation to show the feasibility of the technique. Finally, Section 5 discusses the paper's main conclusions and presents further actions.

2. Temperature determination

In G.984 [8], ranging is performed during ONU activation, in particular, during the Ranging state (O4). To emulate that each ONU is at an equal distance from the OLT, an equalization delay (EqD) for each ONU is required. This equalization delay is measured in bits, and its value

can be obtained from the OLT management interface. The round trip delay (RTD) can be derived as given by

$$RTD_i = T_{eqd} - EqD_i = t_i^{ds} + R_{sp}Time + t_i^{us} \quad (1)$$

where T_{eqd} is the zero-distance EqD, which is the offset between the downstream frame and the desired reception of the upstream frame at the OLT; $t_i^{ds}$and t_i^{us} are the propagation delay in downstream (i.e. at 1490 nm) and upstream (i.e. at 1310 nm), respectively; and $R_{sp}Time$ is the ONU processing time which is $35 \pm 1\ \mu s$. The propagation delay is affected by temperature changes through the dependence of the index of refraction with temperature, (2) [9-12]. This dependence arises mainly from the thermo-optic coefficient, $\frac{dn}{dT}$, of silica since it is one order magnitude larger than thermal expansion [12]. In turn, the thermooptic coefficient arises from changes in the electronic polarizability of the material with temperature. As the temperature of the fiber increases, the thermal energy disrupts the equilibrium position of electrons, causing alterations in the optical properties of silica.

$$n = n_0\left(1 + \frac{dn}{dT}T + \frac{d^2n}{dT^2}T^2 + \cdots\right) \quad (2)$$

Through this dependence, temperature changes can be estimated from EqD readings in time:

$$\Delta RTT = \frac{L}{c}(n_{ds} + n_{us})\left(\frac{dn}{dT}\langle\Delta T\rangle + \frac{d^2n}{dT^2}\langle\Delta T\rangle^2 + \cdots\right) \quad (3)$$

Thus, changes in the spatial average of the environmental temperature along the fiber link can be estimated from changes in EqD for a linear thermo-optic coefficient as:

$$\langle\Delta T\rangle = \frac{\Delta RTT \cdot c}{\frac{dn}{dT}(n_{ds}+n_{us})}\frac{1}{1000} \quad \left[\frac{℃}{km}\right] \quad (4)$$

Different values of the linear thermooptic coefficient (dn/dT) for standard singlemode fiber (ITU-T G.652) can be found in the literature. A typical value for G.652 can be around $7{\cdot}10^{-6}$ K^{-1}, but reported values go from $5{\cdot}10^{-6}$ K^{-1} up to $30{\cdot}10^{-6}$ K^{-1} [3]. Most ITU FTTH standards calculate the EqD value accurately to a single symbol period with respect to the nominal upstream line rate, i.e. 0.8 ns in G.984. Thus, temperature resolution can vary from $16\ ℃/km$ to $2\ ℃/km$. Equation 4 shows that there is a tradeoff between temperature and spatial resolution. However, it can be compensated by integrating information from several fiber trees that can overlap.

In addition, the actual refraction index of the deployed fiber is also unknown. Estimations [1] point out to a variability of $\pm 0.000017 \cdot \left(t_i^{ds} + t_i^{us}\right) = \pm 0.000017 \cdot RTT$, where *RTT* is the round trip time of the fiber. Thus, it has a lower impact on temperature estimation.

To get absolute temperature values, a calibration will be needed to relate an EqD value, with a particular refraction index of the fiber. This information will be combined with the knowledge that the operator has on the type of fiber through its network. The thermal isolation of the cable protection layers can also distort the relation between the internal temperature of the fiber and the external environmental temperature.

The EqD calculation process is carried out during ONU activation. However, it is also performed in-service. The OLT monitors the arrival time of upstream transmission and makes small corrections on EqD without repeating the ranging process. This in-service EqD adjustment, through PLOAM message #21, *Ranging Adjustment*, is done at the request of the

OLT. The OLT maintains two drift thresholds to trigger this update. The most stringent is DoW (Drift of Window) that G.984.3 recommends keeping at ± 4 bits.

To allow regular temperature measurements, the DoW threshold of relevant PON trees should be lowered through firmware modification. The delay resolution from EqD measurements can be enhanced by averaging EqD values obtained in a short time window. Additionally, FTTH networks can show a high density of ONUs per km^2. This can be exploited to reduce the variability of the delay estimation by averaging the values obtained from several close ONUs.

3. Network segmentation and temperature mapping

The information retrieved from PLOAM can be leveraged to build temperature maps. To do so, an existing FTTH network, with any split ratio, is conceptually partitioned into segments. The goal is to combine the readings from several ONUs to infer the approximate average environmental temperature of each segment of the feeder link, although the delay readings are made over concatenations of segments. This process is carried out without modifying the network topology or disrupting data transmission. This benefits from the fact that FTTH networks have long feeder cables with short drops to the subscribers to reduce installation costs. Given the dense deployment of FTTH, there is potential for a good spatial resolution.

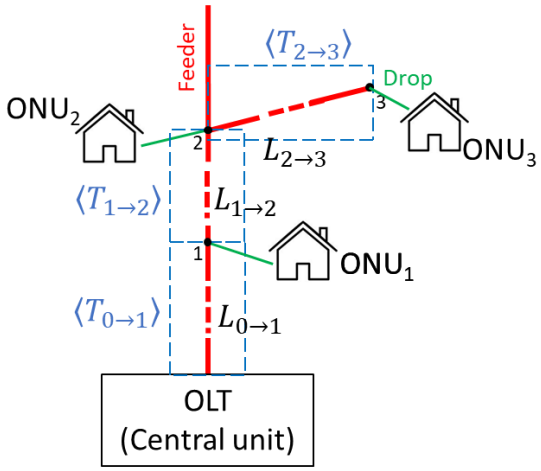

Fig. 1. Concept of segmentation of a conventional FTTH feeding cable, where $\langle T_{i\to j}\rangle$ is the average temperature of the segment going from point i to j which has length $L_{i\to j}$.

To develop a temperature map, relevant ONUs are probed, and the measurements are processed to leverage the tree topology of the access network. An example of an ideal case with a possible segmentation is shown in Fig. 1. The diagram shows how some of the ONUs of a conventional PON network, as deployed to provide FTTH communication services, are used to probe temperature information across the link. In this example, it is seen that the average temperature from the OLT to ONU$_1$ depends only on segment $L_{0\to1}$,

$$\langle \Delta T_{0\to1}\rangle = \frac{1}{L_{0\to1}} \int_0^{L_{0\to1}} T(z)dz \tag{5}$$

where $T(z)$ is the spatial evolution of environmental temperature along the fiber. Changes in the average temperature along the segment are given by (4).

The average temperature in segment $L_{1\to2}$ can be calculated from the value of the previous segment. The average temperature until ONU_2 can be expressed as:

$$\langle \Delta T_{0\to2} \rangle = \frac{1}{L_{0\to2}} \int_0^{L_{0\to2}} T(z)dz = \frac{\langle \Delta T_{0\to1} \rangle \cdot L_{0\to1} + \langle \Delta T_{1\to2} \rangle \cdot L_{1\to2}}{L_{0\to2}} \quad (6)$$

Knowing $\langle \Delta T_{0\to1} \rangle$ from the previous step and assuming both measurements are carried out close enough in time, it is possible to infer $\langle \Delta T_{1\to2} \rangle$ from the EqD variation measured at ONU_2. This procedure can be executed iteratively to estimate the average temperature variation for each segment or a system of equations can also be defined, as shown in (7),

$$\begin{pmatrix} 1 & 0 & \cdots & 0 \\ \frac{L_{0\to1}}{L_{0\to1}+L_{1\to2}} & \frac{L_{1\to2}}{L_{0\to1}+L_{1\to2}} & \cdots & 0 \\ \vdots & \vdots & \vdots & \vdots \\ \frac{L_{0\to1}}{\sum L_{k-1\to k}} & \frac{L_{1\to2}}{\sum L_{k-1\to k}} & \cdots & \frac{L_{n-1\to n}}{\sum L_{k-1\to k}} \end{pmatrix} \begin{pmatrix} \langle \Delta T_{0\to1} \rangle \\ \langle \Delta T_{1\to2} \rangle \\ \vdots \\ \langle \Delta T_{n-1\to n} \rangle \end{pmatrix} = \begin{pmatrix} \langle \Delta T_{0\to1} \rangle \\ \langle \Delta T_{0\to2} \rangle \\ \vdots \\ \langle \Delta T_{0\to n} \rangle \end{pmatrix} \quad (7)$$

where $\langle \Delta T_{i\to j} \rangle$ represents the average temperature of the segment between points i and j.

An error is introduced if the intermediate ONUs are far from the common link, followed by subsequent segments. However, the large number of ONUs in a network can help to reduce this error.

3.1 Simulation results

Numerical simulations have been carried out in MATLAB to assess the potential of building a temperature map. Figure 2 shows an example of a temperature profile for a simplified network as the one shown in Fig. 1. The linear link has been discretized into 1000 bins. The temperature of each bin has been assigned following a continuous equation to model an arbitrary temperature profile and the continuous nature of temperature distribution. Then, the accumulated effect of temperature on time delay has been modeled following Eq. 3. From the reading of the RTT at each ONU, the inverse problem has been solved to retrieve the temperature profile. Fig. 2 shows the arbitrary temperature spatial profile and its retrieval from average delay measurements in several segments, assuming a network where 6 linearly placed ONUs, each 2 km apart, have been used for temperature retrieval. The blue solid line shows the average temperature in each segment retrieved with the iterative algorithm. As can be seen, the problem is similar to sample and hold interpolation in Analog-to-digital converters (ADC). The black dashed line shows a temperature profile reconstruction through interpolation with splines. Interpolation should be carried out with smooth functions since temperature changes are adiabatic.

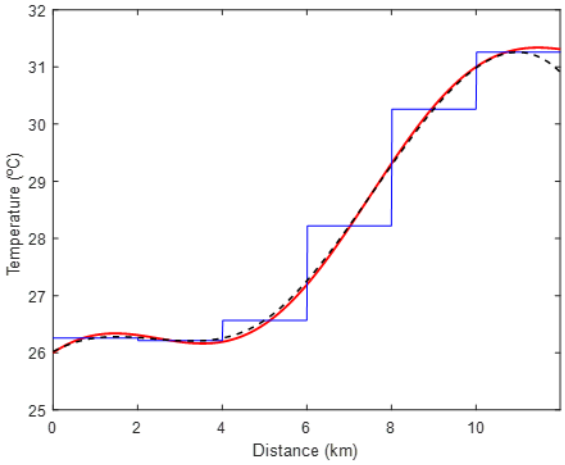

Fig. 2. Simulation of the reconstruction of a given temperature spatial profile (red) from ONU measurements assuming ONU equispaced at 2 km. The blue line shows the average temperature of the segment, and the dashed black line shows a cubic spline interpolation of averaged temperature values.

In Fig. 2, reconstruction was carried out under ideal conditions. A source of error arises from the finite resolution in retrieving the time delay from the finite quantification of the EqD. However, PON topology can be exploited to reduce this uncertainty since it allows averaging delay measurements from a set of close ONUs. This can be combined with time averaging through fast interrogating each ONU to take advantage of the slow nature of temperature changes. Fig. 3 shows the effect of having a finite resolution in EqD on the temperature retrieval process. The figure shows the impact of having an error of 1 and 4 bits in G.984 on the temperature profile of Fig. 2 and how time/space averaging can be used to ease this limitation. In particular, for these simulations, 160 EqD readings were averaged, considering a take ratio of 50% for the conventional value of 64 ONUs per tree and 5 interrogations per ONU. It can be seen how the standard deviation of the temperature error due to uncertainty in the delay estimation is reduced as the fiber length grows and also that for an error of 4 bits, the chosen averaging strategy might be insufficient. The temperature resolution is enhanced with longer fiber lengths since Eq. (4) shows a tradeoff between temperature and spatial resolution. However, a more precise value can be extracted by raising the number of interrogations per ONU and averaging or by using high-speed PON standards with shorter bit lengths.

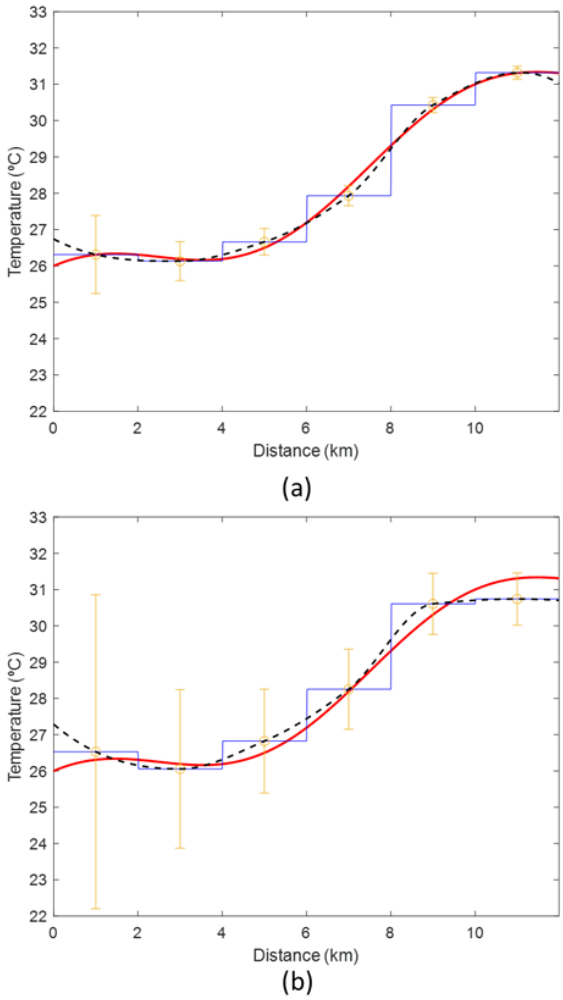

Fig. 3. Simulation results for the enhancement of temperature retrieval from averaging of time delay values for finite length EqD using interpolation by a piecewise cubic Hermite interpolating polynomial: time delay error (a) 1bits and (b) 4 bits.

4. Experimental results

4.1Temperature determination

The first step in the process is determining temperature with PON equipment. The potential of commercial G.984 components for temperature estimation has been previously researched [7]. Experiments based on a fiber coil immersed in a water bath connected to an OLT and ONT were carried out to study the relationship between changes in EqD and temperature variation.

Figure 4 shows the results of the experiment. In particular, a coil of ITU-T G.657.A1 fiber used for FTTH aerial drops, with a 250 µm tight buffer embedded in a plastic cable jacket, was used. Its length was 2940 meters. An OLT, ZTE C320, and one ONT, ZTE F601, were connected through the fiber. The water bath was heated to various temperatures, and the water temperature was continuously monitored using a thermometer. Each value in Fig. 3 is the median of five EqD recordings after forcing ONU activation since the OLT is a commercial

model with limited access to the firmware. It shows that temperature can be inferred from OLT readings after calibration. The relation can be assumed to be linear with the goodness of fit parameter R^2=0.946, which agrees with a linear thermooptic coefficient.

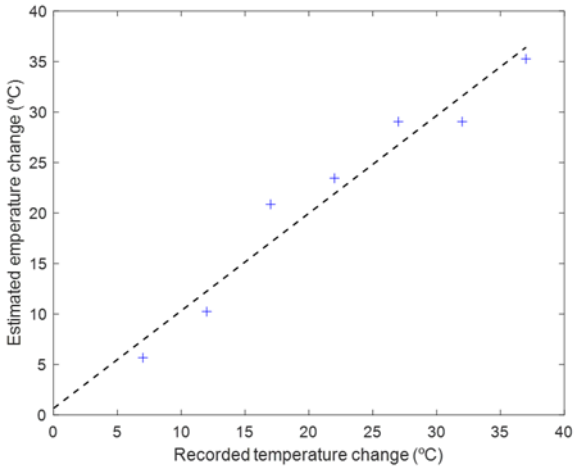

Fig. 4. Average temperature measurement using a ZTE C320 OLT and a ZTE F601 ONT with a spool of 2940 meters of G.657.A1 fiber and linear fit.

4.2 Temperature mapping

Preliminary tests to prove the concept of temperature mapping were carried out in a commercial G.984 network with an aerially deployed optical distribution network. Tests were done while the network was operational. Five consecutive readings of the EqD value of each ONT were recorded at two different times of the day with different environmental temperatures, 21ºC and 27ºC, respectively. These values were average values for the whole area obtained from the local weather service. Three subscribers relatively close to the main feeding cable were selected and probed. The median of the five consecutive EqD readings was used to get the difference in bits. This difference was associated with a temperature change along the optical distribution network. Table 1 summarizes the EqD values for three ONUs. From the difference in EqD values, a temperature difference can be estimated.

Table 1. EqD values at two environmental temperatures in a commercial FTTH network in operation

Subscriber	Link	Link length	21ºC	27ºC	Estimated temperature difference (ºC)
			Median EqD	Median EqD	
ONU#1	0 → 1	1021 m	244350	244348	5±3.1
ONU#2	0 → 2	2002 m	229679	229674	5.9±1.5
ONU#3	0 → 3	3000 m	221829	221823	5.8±0.7

A temperature map can be created based on these temperature changes. A calibration is used to assign a temperature value of the link to the EqD reading of an ONU since the thermooptic coefficient of the fiber is unknown. Table 2 shows the average temperature estimations in the different segments of the link, in this case, $\langle T_{0\to1}\rangle$, $\langle T_{1\to2}\rangle$ and $\langle T_{2\to3}\rangle$, from the values of Table 1, which are the average of five measurements, and following the procedure described in

Section 3. An example of a map is shown in Fig. 5 where the three probed ONUs allow for the division of the PON into three segments and, therefore, three temperature averages can be estimated.

Table 2. Estimated temperature difference from each link section

Link		Temperature difference (ºC)
$0 \rightarrow 1$	$\langle \Delta T_{01} \rangle$	5 ± 3.1
$1 \rightarrow 2$	$\langle \Delta T_{12} \rangle$	7.1 ± 1.7
$2 \rightarrow 3$	$\langle \Delta T_{23} \rangle$	5.6 ± 2.3

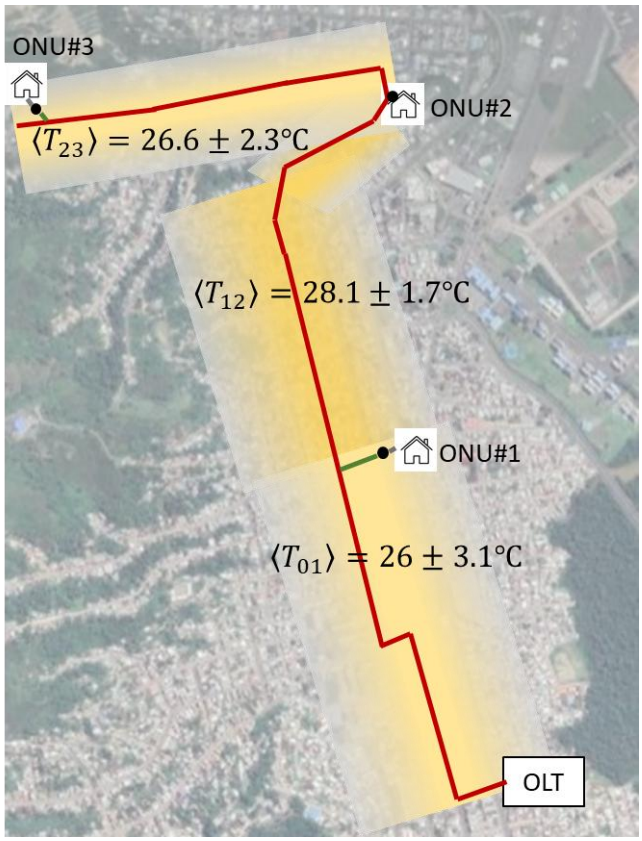

Fig. 5. Example of temperature mapping derived from PLOAM information with three segments. The red line represents a cable with 48 fibers; the green one is a cable with six fibers; and the grey one a cable of two fibers, one active and one in reserve. The NAP (Network Access Point), with the second splitter 1:8, serving the ONUs used for monitoring, is represented with a black dot.

This concept can be extended to combine the information from many trees of the PON network and integrate this information to obtain maps of temperature differences in cities and rural areas.

5. Conclusion

A new method to build maps for environmental temperature derived from the management information of FTTH networks used to provide a communication service has been proposed. It has been shown that the round-trip time (RTT) of the data across the PON tree can be leveraged to retrieve sensing data. This information is available to telecom operators, which would only

need to perform a firmware upgrade to allow for this new kind of environmental sensing using already deployed infrastructure. This management information can be leveraged to provide environmental data on cities or suburban/rural areas, contributing to better weather forecasts and enhanced monitoring of heat waves in cities.

The preliminary results presented here suggest the feasibility of this new application. Although demonstrated for G.984, high-speed PON standards (G.987, G.9807, G.9804) are better suited to provide enhanced temperature resolution. Further work would include tests over wider areas and a larger number of users to assess the potential of the technique and a comparison of the results with simultaneous internal information from meteorological services or satellite data. It would also be worth studying methods to reduce the uncertainty of the delay obtained from the OLT and analyzing the effect of the protection layers of the fiber cable on the temperature isolation as well as on the errors in the estimation of air temperature due to the sun irradiation on the black cables.

This work might provide a new application for the hundreds of thousands of km of deployed optical fibers worldwide and make use of information available to telecom operators with no significant additional cost.

Acknowledgements. The authors would like to acknowledge María Yolanda Luna and José Ángel Núñez from the Spanish Meteorological Agency (AEMET) for helpful discussions.

Disclosures. The authors declare no conflicts of interest.

Data availability. Data underlying the results presented in this paper are not publicly available at this time but may be obtained from the authors upon reasonable request.

References

1. T. Wild, V. Braun and H. Viswanathan, "Joint Design of Communication and Sensing for Beyond 5G and 6G Systems," IEEE Access, vol. 9, pp. 30845-30857, 2021, doi: 10.1109/ACCESS.2021.3059488.
2. J. A. Zhang et al., "Enabling Joint Communication and Radar Sensing in Mobile Networks—A Survey", IEEE Communications Surveys & Tutorials, vol. 24, no. 1, pp. 306-345, First quarter 2022, doi: 10.1109/COMST.2021.3122519.
3. Z. Zhan, M. Cantono, V. Kamalov, A.Mecozzi, R. Müller, S. Yin, J.C. Castellanos, “Optical polarization-based seismic and water wave sensing on transoceanic cables”, Science, vol. 371, no. 6532, pp. 931-936, Feb. 2021. doi: 10.1126/science.abe6648.
4. M. Mazur, J.C. Castellanos, R. Ryf, E. Börjeson, T. Chodkiewicz, V. Karmalov, S. Yin, N.K. Fontaine, H. Chen, L. Dallachiesa, S. Corteselli, P. Copping, J. Gripp, A. Mortelette, B. Kowalski, R. Dellinger, D.T. Neilson, P. Larsson-Edefors, “Transoceanic phase and polarization fiber sensing using real-time coherent transceiver”, 2022 Optical Fiber Communications Conference (OFC 2022), M2E.2, San Diego (USA), 6-10 March 2022.
5. P. Lu, N. Lalam, M. Badar, B. Liu, B.T. Chorpening, M.P. Buric, P.R. Ohodnicki, “Distributed optical fiber sensing: Review and perspective”, Applied Physics Reviews, vol. 6, no. 4, 041302, Dec. 2019.
6. X. Li, G. Dick, C. Lu, M. Ge, R. Nilsson, T. Ning, J. Wickert, H. Schuh, “Multi-GNSS Meteorology: Real-Time Retrieving of Atmospheric Water Vapor From BeiDou, Galileo, GLONASS, and GPS Observations”, IEEE Trans. Geoscience and Remote Sensing, vol. 53, no. 12, pp. 6385-6393, Dec 2015.
7. C. Salgado-Cazorla, B. Vidal, “Towards Costless Temperature Monitoring through PLOAM Information in TDMA PON Networks”, 2023 Optical Fiber Communications Conference (OFC 2023), JThA71, San Diego (USA), 5-9 March 2023.
8. Gigabit-capable passive optical networks (G-PON): Transmission convergence layer specification, ITU G.984.3, 2014.
9. A.H. Hartog, A.J. Conduit, D.N. Payne, “Variation of pulse delay with stress and temperature in jacketed and unjacketed optical fibres”, Opt Quant Electron 11, 265–273 1979.
10. P.E. Dupouy, M. Büchner, P. Paquier, G. Trénec, J. Vigué, "Interferometric measurement of the temperature dependence of an index of refraction: application to fused silica", Appl. Optics, 49 678-682, 2010.
11. M. Bousonville, M.K. Bock, M. Felber, T. Ladwig, T. Lamb, C. Sydlo, H. Schlarb, S.A. Schulz, S.G. Hunziker, P. Kownacki,. “New phase stable optical fiber”, Proceedings of BIW2012, Newport News, USA, 2012.
12. Z.Y. Wang, Q. Qiu, S.J. Shi, “Temperature dependence of the refractive index of optical fibers”, Chi. Phys. B, 23, 034201 2014.